

See discussions, stats, and author profiles for this publication at: <https://www.researchgate.net/publication/40805086>

Interaction Forces between Microsized Silica Particles and Weak Polyelectrolyte Brushes at Varying pH and Salt Concentration

ARTICLE in LANGMUIR · MAY 2010

Impact Factor: 4.46 · DOI: 10.1021/la904103z · Source: PubMed

CITATIONS

32

READS

31

6 AUTHORS, INCLUDING:



Alla Synytska

Leibniz Institute of Polymer Research Dresden

57 PUBLICATIONS 983 CITATIONS

SEE PROFILE



Petra Uhlmann

Leibniz Institute of Polymer Research Dresden

83 PUBLICATIONS 1,179 CITATIONS

SEE PROFILE



Mahdy Mohammed Elmahdy

Mansoura University

17 PUBLICATIONS 332 CITATIONS

SEE PROFILE



Friedrich Kremer

University of Leipzig

68 PUBLICATIONS 860 CITATIONS

SEE PROFILE

Interaction Forces between Microsized Silica Particles and Weak Polyelectrolyte Brushes at Varying pH and Salt Concentration

Astrid Drechsler,^{*,†} Alla Synytska,[†] Petra Uhlmann,[†] Mahdy M. Elmahdy,^{‡,§} Manfred Stamm,[†] and Friedrich Kremer[‡]

[†]Leibniz Institute of Polymer Research Dresden, Hohe Str. 6, 01069 Dresden, Germany,

[‡]Institute of Experimental Physics I, Leipzig University, Linnéstr. 5, 04103 Leipzig, Germany, and

[§]Department of Physics, Mansoura University, Mansoura 35516, Egypt

Received October 28, 2009. Revised Manuscript Received December 15, 2009

The AFM colloidal probe technique was used to measure the interaction between microsized silica spheres and annealed polyelectrolyte brushes made of poly(acrylic acid) (PAA) and poly(2-vinyl pyridine) (P2VP) in KCl solutions of various pH values and salt concentrations. The interaction energy showed a distance dependence that was affected strongly by the swelling and the electric properties of the brushes. Between PAA brushes and silica particles, a repulsive interaction has been observed for all pH values and salt concentrations reflecting the swelling of the brush with varying pH value and the transition from osmotic to salted brush regime with increasing KCl concentration. Force measurements between P2VP brushes and silica particles revealed a much more complex behavior: a steric repulsion by the swollen brush at low pH values, a complex interplay of attractive and repulsive forces at intermediate pH values and a short-ranged attraction between the collapsed brush and the silica particle at basic pH values and high salt concentrations. The results are interpreted in comparison with the Alexander de Gennes model and zeta potential and ellipsometric measurements.

1. Introduction

Polymer brushes, i.e., thin layers of polymer chains grafted by one end to a solid substrate, are promising materials for the design of surfaces with advanced properties. They may change their surface properties in response to external stimuli as, e.g., the solvent quality of the surrounding medium or the temperature, and have been demonstrated to provide a wide range of different properties for numerous applications.¹

Polyelectrolyte brushes, i.e., brushes of charged polymers, are a particular case of polymer brushes. Two types of polyelectrolyte brushes are distinguished: quenched brushes made of strong polyelectrolytes, which are completely dissociated at all pH values, and annealed brushes consisting of weak polyelectrolytes that dissociate only at certain pH values.² Polyelectrolyte brushes change their conformation and surface properties as charge or wettability in response to a variation of the salt concentration of a surrounding aqueous solution. For annealed polyelectrolyte brushes, additionally the pH value of the solution governs the properties of the brush.²

These switching effects are regarded as very important for the design of biomaterial interfaces³ and have found numerous

applications in the field of controlled protein adsorption,^{4–16} the design of microfluidic devices,¹⁷ responsive wetting,^{18,19} lubrication,^{20,21} sensors,^{22–25} immobilization or controlled motion of nanoparticles,^{26–30} and smart colloids.^{31,32} On the other hand, the interaction of colloidal particles covered by polyelectrolyte

- (10) Wittemann, A.; Haupt, B.; Ballauff, M. *Z. Phys. Chem NF* **2007**, *221*, 113.
- (11) Synytska, A.; Diez, S.; Stamm, M.; Ionov, L. *Langmuir* **2007**, *23*, 5205.
- (12) Ionov, L.; Synytska, A.; Diez, S. *Adv. Funct. Materials* **2008**, *18*, 1501.
- (13) Ionov, L.; Houbenov, N.; Sidorenko, A.; Stamm, M.; Minko, S. *Biointerphases* **2009**, *4*, FA45.
- (14) Burkert, S.; Bittrich, E.; Eichhorn, K.-J.; Uhlmann, P.; Stamm, M. **2009**, *Biomacromolecules*, submitted.
- (15) de Vos, W. M.; Biesheuvel, P. M.; de Keizer, A.; Kleijn, J. M.; Cohen Stuart, M. A. *Langmuir* **2008**, *24*, 65754.
- (16) de Vos, W. M.; Leermakers, F. A. M.; de Keizer, A.; Cohen Stuart, M. A.; Kleijn, J. M. *Langmuir* [Online early access] DOI: 10.1021/la902079u
- (17) Ionov, L.; Houbenov, N.; Sidorenko, A.; Stamm, M.; Minko, S. *Adv. Funct. Mater.* **2006**, *16*, 1153.
- (18) Motornov, M.; Minko, S.; Eichhorn, K.-J.; Nitschke, M.; Simon, F.; Stamm, M. *Langmuir* **2003**, *19*, 8077.
- (19) Minko, S.; Müller, M.; Motornov, M.; Nitschke, M.; Grundke, K.; Stamm, M. *J. Am. Chem. Soc.* **2003**, *125*, 3896.
- (20) Dunlop, I. E.; Briscoe, W. H.; Titmuss, S.; Sakellariou, G.; Hadjichristidis, N.; Klein, J. *Macromol. Chem. Phys.* **2004**, *205*, 2443.
- (21) Dunlop, I. E.; Briscoe, W. H.; Titmuss, S.; Jacobs, R. M. J.; Osborne, V. L.; Edmondson, S.; Huck, W. T. S.; Klein, J. *J. Phys. Chem. B* **2009**, *113*, 3947.
- (22) Ionov, L.; Sapra, S.; Synytska, A.; Rogach, A. L.; Stamm, M.; Diez, S. *Adv. Mater.* **2006**, *18*, 1453.
- (23) Gupta, S.; Uhlmann, P.; Agrawal, M.; Chapuis, S.; Oertel, U.; Stamm, M. *Macromolecules* **2008**, *41*, 2874.
- (24) Kokoz, B.; Korneev, K. G.; Luzinov, I. *ACS Appl. Mater. Interfaces* **2009**, *1*, 575.
- (25) Chumanov, G.; Sokolov, K.; Cotton, T. M. *J. Phys. Chem.* **1996**, *100*, 5166.
- (26) Malynych, S.; Luzinov, I.; Chumanov, G. *J. Phys. Chem. B* **2002**, *106*, 1280.
- (27) Santer, S.; Rühle, J. *Polymer* **2004**, *45*, 8279.
- (28) Mei, Y.; Sharma, G.; Lu, Y.; Ballauff, M.; Drechsler, M.; Irrgang, T.; Kempe, R. *Langmuir* **2005**, *21*, 12229.
- (29) Gupta, S.; Uhlmann, P.; Agrawal, M.; Lesnyak, V.; Gaponic, N.; Eychmüller, A. *J. Mater. Chem.* **2008**, *18*, 214.
- (30) Gupta, S.; Agrawal, M.; Uhlmann, P.; Simon, F.; Oertel, U.; Stamm, M. *Macromolecules* **2008**, *41*, 8152.
- (31) Ballauff, M.; Lu, Y. *Polymer* **2007**, *48*, 1815.
- (32) Berger, S.; Synytska, A.; Ionov, L.; Eichhorn, K.-J.; Stamm, M. *Macromolecules* **2008**, *41*, 9669.

*E-mail: drechsler@ipfdd.de.

(1) Advincula, R. C.; Brittain, W. J.; Caster, K. W.; Rühle, J., Eds. *Polymer Brushes. Synthesis, Characterization, Applications*; Wiley-VCH: Weinheim, 2004.

(2) Israëls, R.; Leermakers, F. A. M.; Fleer, G. J. *Macromolecules* **1994**, *27*, 3087.

(3) Galaev, I. Y.; Mattiasson, B. *Trends Biotechnol.* **1999**, *17*, 335.

(4) Wittemann, A.; Haupt, B.; Ballauff, M. *Phys. Chem. Chem. Phys.* **2003**, *5*, 1671.

(5) Czeslik, C.; Jackler, G.; Hazlett, T.; Gratton, E.; Steitz, R.; Wittemann, A.; Ballauff, M. *Phys. Chem. Chem. Phys.* **2004**, *6*, 5557.

(6) Ionov, L.; Stamm, M.; Diez, S. *Nano Lett.* **2005**, *5*, 1910.

(7) Houbenov, N.; Ionov, L.; Minko, S.; Stamm, M. *Polym. Prepr.* **2005**, *46*, 1229.

(8) Wittemann, A.; Ballauff, M. *Phys. Chem. Chem. Phys.* **2006**, *8*, 5269.

(9) Uhlmann, P.; Houbenov, N.; Brenner, N.; Grundke, K.; Burkert, S.; Stamm, M. *Langmuir* **2007**, *23*, 57.

brushes with charged surfaces can be controlled.^{33,34} Polyelectrolytes as binding media have the great advantage that each molecule contains a large number of charged groups resulting in a high binding strength provided by electrostatic interactions. In the dissociated state, charged groups interact electrostatically with charged surfaces, but they also may form hydrogen bonds with polar species.²⁶

The interesting behavior of annealed polyelectrolyte brushes arises from the fact that the fraction of dissociated monomers depends on the pH and the salt concentration of the surrounding medium, as well as on the grafting density of the chain and the distance to the grafting plane. Detailed theoretical studies have been presented by Pincus,^{35,36} Borisov, Zhulina and Birshtein,^{37–39} and Leermakers et al.^{2,16,40}

Their calculations showed that at low salt concentrations the proton concentration in the brush is significantly higher than in the bulk solution while the overall counterion density is low. Thus, each ion contributes on the order of $k_B T$ to the osmotic pressure in the brush. This regime is referred to as the osmotic brush regime. The average degree of dissociation increases with increasing (for polyacids) or decreasing (for polybases) pH value and ion density of the surrounding solution. On the other hand, the degree of dissociation decreases with increasing grafting density of the brush. At sufficiently high grafting densities, the brush may appear electrically neutral. The brush height which is a result of steric and conformational but mostly of electrostatic interactions between the charged brush molecules thus increases in the osmotic brush regime with increasing pH and ion density of the solution, and it may decrease with increasing grafting density. Once the ion concentration in the surrounding solution reaches the ion concentration in the brush, the brush enters the salted brush regime. In this regime, the charges of the brush are increasingly screened by counterions; the brush thickness decreases with increasing ionic strength of the solution. As a result, the thickness of annealed brushes shows a maximum at intermediate salt concentrations.^{41–45}

For many applications, the interaction forces between polyelectrolyte brushes and colloidal particles in aqueous solutions of varying pH value and ion concentration are of great interest. From the literature, force–distance measurements between a wide variety of polyelectrolyte brushes are known. Most of them were done in systems where both surfaces are covered with identical brushes. They were performed using the surface force

apparatus,^{46–50} the surface force balance,^{20,21} and the AFM colloidal probe technique.^{51–57} Forces between two micro-sized particles carrying polyelectrolyte brushes were determined very recently by optical tweezers^{58,59} and by microsurface potential measurements.⁶⁰

The forces acting between annealed polyelectrolyte brushes reflect the conformational changes of the brush with varying pH and salt concentration. In the pioneering study of Kurihara et al.,⁴⁶ the forces between adsorbed poly-(methacrylic acid) brushes were measured. Since the grafting density of the adsorbed brushes was rather low, repulsive steric and electrostatic force contributions were observed. The range and strength of the steric interaction increased both with increasing pH and increasing salt concentration. Force measurements between thin adsorbed polyelectrolyte layers revealed a behavior that could be described completely by the DLVO theory.⁵¹ More recent studies^{47–50,56,57} with more densely grafted brushes showed a purely steric repulsion. The force–distance curves obtained by these measurements could be modeled by the Alexander de Gennes model, which was originally developed for uncharged brushes. On the basis of a steplike profile of the brush, the repulsive pressure between two identical brushes P_{symm} is described as a function of the area per chain s , the brush thickness L , and the distance D .⁶¹

$$P_{\text{symm}}(D) = \frac{k_B T}{s^3} \left[\left(\frac{2L}{D} \right)^{9/4} - \left(\frac{D}{2L} \right)^{3/4} \right] \quad (1)$$

k_B is the Boltzmann constant and T the temperature. Calculations by Milner et al.⁶² (the MWC model) assume a parabolic volume fraction profile of the brush. The pressure–distance profile differs, however, only slightly from that obtained by eq 1.⁵⁷

Only a few studies dealt with force measurements between bare micro-sized particles and polyelectrolyte brushes. They were done using the AFM colloidal probe technique^{63,64} that measures the force between a colloid glued to a tipless AFM cantilever spring and a flat surface as a function of the distance. Block and Helm⁵⁷ compared the interaction between a flat poly(styrene sulfonate) (PSS) brush and silica spheres with and without adsorbed PSS. PSS is a strong polyelectrolyte and forms a quenched brush that does not show a pronounced pH dependence of the brush thickness as annealed brushes do.⁴³ The forces between the swollen brushes agreed very well both with the Alexander de Gennes model and with the MWC model. The interactions between a swollen brush and the bare sphere could be modeled using a modified

- (33) Mei, Y.; Wittemann, A.; Sharma, G.; Ballauff, M.; Koch, T.; Gliemann, H.; Horbach, J.; Schimmel, T. *Macromolecules* **2003**, *36*, 3452.
 (34) Gliemann, H.; Mei, Y.; Ballauff, M.; Schimmel, T. *Langmuir* **2006**, *22*, 7254.
 (35) Pincus, P. *Macromolecules* **1991**, *24*, 2912.
 (36) Ross, R.; Pincus, P. *Macromolecules* **1992**, *25*, 2177.
 (37) Borisov, O. V.; Birshtein, T. M.; Zhulina, E. B. *J. Phys. II (France)* **1991**, *1*, 521.
 (38) Zhulina, E. B.; Borisov, O. V.; Birshtein, T. M. *J. Phys. II (France)* **1992**, *2*, 63.
 (39) Zhulina, E. B.; Birshtein, T. M.; Borisov, O. V. *Macromolecules* **1995**, *28*, 1491.
 (40) Leermakers, F. A. M.; Ballauff, M.; Borisov, O. V. *Langmuir* **2007**, *23*, 3937.
 (41) Ahrens, H.; Förster, S.; Helm, C. A. *Phys. Rev. Lett.* **1998**, *81*, 4172.
 (42) Currie, E. P. K.; Sieval, A. B.; Fleer, G. J.; Cohen Stuart, M. A. *Langmuir* **2000**, *16*, 8324.
 (43) Guo, X.; Ballauff, M. *Phys. Rev. E* **2001**, *64*, 051406.
 (44) Konradi, R.; Rühle, J. *Macromolecules* **2005**, *38*, 4345.
 (45) Wu, T.; Gong, P.; Szeifer, I.; Vlček, P.; Šubr, V.; Genzer, J. *Macromolecules* **2007**, *40*, 8756.
 (46) Kurihara, K.; Kunitake, T.; Higashi, N.; Niwa, M. *Langmuir* **1992**, *8*, 2087.
 (47) Abraham, T.; Giasson, S.; Gohy, J. F.; Jérôme, R. *Langmuir* **2000**, *16*, 4286.
 (48) Hayashi, S.; Abe, T.; Higashi, N.; Niwa, M.; Kurihara, K. *Langmuir* **2002**, *18*, 3932.
 (49) Balastre, M.; Li, F.; Schorr, P.; Yang, J.; Mays, J. W.; Tirrell, M. V. *Macromolecules* **2002**, *35*, 9480.
 (50) Liberelle, B.; Giasson, S. *Langmuir* **2008**, *24*, 1550.

- (51) Hartley, P. G.; Scales, P. J. *Langmuir* **1998**, *14*, 6948.
 (52) Yamamoto, S.; Ejaz, M.; Tsujii, Y.; Matsumoto, M.; Fukuda, T. *Macromolecules* **2000**, *33*, 5602.
 (53) Yamamoto, S.; Ejaz, M.; Tsujii, Y.; Fukuda, T. *Macromolecules* **2000**, *33*, 5608.
 (54) Feiler, A.; Plunkett, M. W.; Rutland, M. W. *Langmuir* **2003**, *19*, 4173.
 (55) Notley, S.; Biggs, S.; Craig, V. S. J. *Macromolecules* **2003**, *36*, 2903.
 (56) Block, S.; Helm, C. A. *Phys. Rev. E* **2007**, *76*, 030801.
 (57) Block, S.; Helm, C. A. *J. Phys. Chem. B* **2008**, *112*, 9318.
 (58) Domínguez Espinosa, G.; Synytska, A.; Drechsler, A.; Gutsche, C.; Kegler, K.; Uhlmann, P.; Stamm, M.; Kremer, F. *Polymer* **2008**, *49*, 4802.
 (59) Elmahdy, M. M.; Synytska, A.; Drechsler, A.; Gutsche, C.; Uhlmann, P.; Stamm, M.; Kremer, F. *Macromolecules* **2009**, *42*, 9096.
 (60) Schneider, C.; Jusufi, A.; Farina, R.; Li, F.; Pincus, P.; Tirell, M.; Ballauff, M. *Langmuir* **2008**, *24*, 10612.
 (61) de Gennes, P. G. *Macromolecules* **1980**, *13*, 1069.
 (62) Milner, S. T.; Witten, T. A.; Cates, M. E. *Macromolecules* **1988**, *21*, 2610.
 (63) Butt, H.-J. *Biophys. J.* **1991**, *60*, 1438.
 (64) Ducker, W. A.; Senden, T. J.; Pashley, R. M. *Langmuir* **1992**, *8*, 1831.

Alexander de Gennes model:⁶⁵

$$P_{\text{asymm}}(D) = \frac{k_B T}{2s^3} \left[\left(\frac{L}{D} \right)^{9/4} - \left(\frac{D}{L} \right)^{3/4} \right] \quad (2)$$

and adding an electrostatic contribution. Force measurements yield the force F as a function of the distance D between two surfaces. In the case of a sphere of radius R interacting with a flat surface, the force can be converted into a geometry-independent interaction energy by using the Derjaguin approximation:⁶⁶

$$E(D) = F(D)/2\pi R \quad (3)$$

It is obtained theoretically by integrating the pressure between the brush and the particle:⁵⁷

$$E_{\text{asymm}}(D) = \frac{2k_B T L}{35s^3} \left[7 \left(\frac{L}{D} \right)^{5/4} + 5 \left(\frac{D}{L} \right)^{7/4} - 12 \right] \quad (4)$$

This energy profile can be approximated at intermediate surface separations ($0.2 L \leq D \leq 0.9 L$) by an exponentially decaying function.⁵⁷

$$E_{\text{asymm}}(D) = E_0 \exp\left(-\frac{D}{t_1}\right) \quad \text{with} \quad t_1 = \frac{L}{2\pi} \quad (5)$$

Thus, from the decay length t_1 , the brush thickness L can be deduced.

The interactions between polyelectrolyte brushes and micro-sized particles may be much more complex if both surfaces have different electrical charges. The forces between a thin adsorbed layer of highly quaternized poly(2-vinyl pyridine) and a silica sphere changed from a pure attraction at $\text{pH} \leq 5.2$ to pure repulsion at $\text{pH} = 8.8$.⁵¹ Force measurements between different micro-sized particles and a poly(acrylic acid) brush⁶⁷ also showed a pronounced influence of the electrical properties of both surfaces on the sign of the interaction forces. The adsorption of proteins on polyelectrolyte brushes depends strongly on the local charge of both surfaces and on the ionic strength of the surrounding solution.^{6–9,14} Proteins are attracted by polyelectrolyte brushes even if their overall surface charges have the same sign but are released if the ion concentration in the solution is increased.^{4,8,15} This effect has been explained theoretically by charge regulation effects and a charge inhomogeneity of the proteins.^{16,40}

This paper presents in situ AFM force measurements between annealed polyelectrolyte brushes and micro-sized silica particles. Other than proteins, the surface charge of the silica colloids is assumed to be constant over the whole particle surface. A weak polyacid, poly(acrylic acid) (PAA), and a weak polybase, poly(2-vinyl pyridine) (P2VP), are chosen to create brushes of different surface charge and pH-dependent dissociation. Recently, these

materials have been the focus of research on responsive mixed brushes.^{7,11,14,68–71} Ellipsometric investigations of the pH and salt-dependent swelling of PAA brushes are given by Currie et al.⁴² and Wu et al.⁴⁵ Guo et al.⁴³ measured the pH-dependent swelling of PAA-modified latex particles. It was shown that the swelling depends strongly on the grafting density of the brushes. PAA brushes similar to those used in the present study dissociate and swell if the pH exceeds 3.2.^{14,68} Force measurements between adsorbed PAA brushes with a grafting density of about $4.3 \text{ nm}^2/\text{chain}$ yielded a purely steric repulsion that had a maximal range and strength in a 10^{-2} M NaCl solution.⁵⁰ Studies by de Vos et al.^{15,16} showed that the adsorption of proteins on PAA brushes depends strongly on the pH value and ion concentration of the surrounding solution and the grafting density of the brush. P2VP brushes similar to those used in this study dissociate and swell at $\text{pH} < 6.7$.^{11,14,32,68} Notley et al.⁵⁵ found purely repulsive forces between P2VP brushes at $\text{pH} = 3.2$ and $\text{pH} = 4.5$.

In the force measurements presented here, the influence of the pH value and counterion density of the surrounding solution is investigated systematically. Both repulsive and attractive forces acting during the approach of the particle and the adhesion force during the retraction are measured. The results of the force measurements are interpreted on the basis of the zeta potential of the particles and the brushes and compared to force measurements between two like silica spheres covered with comparable PAA and P2VP brushes using optical tweezers.^{58,59} The brush thickness obtained from AFM images and energy-distance data is compared to values obtained by null-ellipsometry.

2. Experimental Section

Preparation of the Brushes. *Materials.* Carboxyl-terminated poly(*tert*-butyl acrylate) (PtBA-COOH, $M_n = 42\,000 \text{ g/mol}$, $M_w = 47\,000 \text{ g/mol}$) and poly(2-vinyl pyridine) (P2VP-COOH, $M_n = 40\,600 \text{ g/mol}$, $M_w = 43\,800 \text{ g/mol}$) synthesized by anionic polymerization, were purchased from Polymer Source, Inc. Polyglycidyl methacrylate (PGMA) ($M_n = 84\,000 \text{ g/mol}$) was synthesized by free radical polymerization of glycidyl methacrylate (Aldrich). Methanesulfonic acid (Fluka) was used without additional purification. Polished silicon wafers (100) with a native silicon oxide layer of a thickness of ca. 1.7 nm were purchased from Silchem Handelsgesellschaft GmbH (Freiberg, Germany) and Wacker-Chemtronics GmbH (Burghausen, Germany). Wafers were washed three times with dichloromethane in an ultrasonic bath for 5 min and afterward in a mixture of water, ammonia solution (25%), and hydrogen peroxide (30%) in volume ratio of 1:1:1 at 60 °C for 1 h. The substrates were rinsed 5–6 times in deionized reagent-grade water and then dried with nitrogen flux.

“Grafting to” Approach. PAA and P2VP brush layers were prepared via a two-step procedure as described elsewhere.^{11,32,72} In brief, a thin layer of PGMA ($\sim 1.5 \text{ nm}$) was deposited by spin coating from 0.01% solution in chloroform and annealed at 110 °C for 10 min. On top, a thin film of PtBA-COOH or P2VP-COOH (2% solution in chloroform) was spin-coated and annealed for 5 h at 150 °C. Ungrafted polymer was removed using Soxhlet extraction in chloroform for 3 h. Finally, PtBA was hydrolyzed with methanesulfonic acid for 5 min yielding poly(acrylic acid) (PAA). Physicochemical characterization of the brushes and force measurements were performed within 3 days after the preparation of the brushes. Longer storage led to contamination and aging effects.

Grafting Density of the Polymer (Γ). The distance between the grafting sites and the thickness of the grafted polymer layer (H) were estimated as described elsewhere.⁶⁹ The thickness

(65) O’Shea, S. J.; Welland, M. E.; Rayment, T. *Langmuir* **1993**, *9*, 1826.

(66) Derjaguin, B. V. *Kolloid-Zeitschr.* **1934**, *69*, 155.

(67) Drechsler, A.; Synytska, A.; Uhlmann, P.; Stamm, M.; Kremer, F. *Polym. Mater. Sci. Eng.* **2009**, *101*, 1301.

(68) Houbenov, N.; Minko, S.; Stamm, M. *Macromolecules* **2003**, *36*, 5897.

(69) Ionov, L.; Houbenov, N.; Sidorenko, A.; Stamm, M. *Langmuir* **2004**, *20*, 9916.

(70) Ionov, L.; Sidorenko, A.; Eichhorn, K. J.; Stamm, M.; Minko, S.; Hinrichs, K. *Langmuir* **2005**, *21*, 8711.

(71) Mikhailova, Y.; Ionov, L.; Rappich, J.; Gensch, M.; Esser, N.; Minko, S.; Eichhorn, K.-J.; Stamm, M.; Hinrichs, K. *Anal. Chem.* **2007**, *79*, 7676.

(72) Synytska, A.; Ionov, L.; Dutschk, V.; Stamm, M.; Grundke, K. *Langmuir* **2008**, *24*, 11895.

of the P2VP and PAA layers were 8 and 5 nm (dry film), respectively, corresponding to a grafting density of 0.12 chains/nm².

Electrolyte Solutions. These have been prepared from 0.1 molar KCl (Bernd Kraft GmbH, Germany), HCl (Titrisol, Merck), and KOH (Fixanal, Riedel-de Haen) solutions with purified water (Purilab Plus, ELGA Lab Water). Since the DI water had pH = 5.8, pH = 6.8 was adjusted by addition of 10⁻⁶ M KOH. The pH value was controlled before each measurement.

Ellipsometry. The thickness of polymer layers in the dry state was measured at $\lambda = 632.8$ nm and an angle of incidence of 70° with a null-ellipsometer in a polarizer compensator-sample analyzer (Multiscopie, Optrel Berlin, Germany) micro-focus ellipsometer as described elsewhere.^{73,74} From the obtained values, we calculated the distance between grafting points $d = (H\rho N_A/M_w)^{-1/2}$, where H is the ellipsometric thickness, ρ is the mass density (for simplicity, we used $\rho = 1$ g/cm³), N_A is the Avogadro's number, and M_w is the molecular weight. The distance between the grafting sites (~ 2.8 nm) is smaller than the unperturbed radius of gyration (R_g) of grafted polymer PAA/or P2VP coils ($R_g \sim 5$ nm) in θ conditions. In a good solvent, the polymer chains are swollen, and the R_g is much larger than under θ conditions. Consequently, the polymer-grafted film exposed to good solvent can be considered as a brush-like layer.⁷⁰

In situ ellipsometric measurements were performed to examine the swelling behavior of the polymer brushes in different pH and ionic strength media. An ellipsometric cell (TSL spectroil B, Hellma, Müllheim, Germany) with thin glass walls, fixed at an angle of 68° from the sample plane, was used. The angle of incidence of the light was set such that its path was normal to the window. An optical four-layer model (silicon substrate with refractive index $n = 3.8705 - j0.0168$, SiO₂ ($n = 1.4598$), PGMA ($n = 1.5250$), and the P2VP or PAA layer thickness with fitted or previously estimated refractive indexes using variable angle multiwavelength ellipsometry) was used to calculate the brush thicknesses from the ellipsometric angles Ψ and Δ . This method has to be regarded as an estimation, since the layer model used to calculate the brush thickness requires flat surfaces with a stepwise change of the refractive index. The surface of a swollen brush is rather a diffuse distribution of molecule end groups. The null ellipsometry results reflect, however, qualitatively well the swelling of the brushes.

Refractive indexes (n) of the thin layers were estimated separately by use of a rotating analyzer type variable angle multiwavelength ellipsometer M-44 (J.A. Woollam Co. Inc. USA) in the wavelength range from 428 to 763 nm. The values of n were extracted at 633 nm and later used in the optical model for the evaluation of the brush thickness in the liquid medium.

Zeta Potential Measurements. The surface potential of the brushes was determined by streaming potential measurements carried out with the Electrokinetic Analyzer (EKA) by Anton Paar GmbH (Graz, Austria) using a special rectangular cell for small flat pieces. Details of the measuring technique and the used device are reported in refs 75,76. Two small pieces of a brush-coated silicon wafer (10 × 20 mm²) were arranged parallel face to face to build a streaming channel inside the cell. The measuring electrolyte was circulated through this channel. The streaming potential vs pressure loss was measured by means of Ag/AgCl

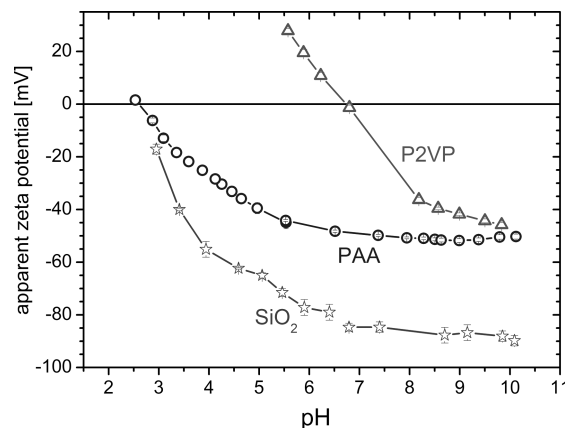


Figure 1. Apparent zeta potential of PAA brushes (circles), P2VP brushes (triangles), and microsilica spheres (stars) in 10⁻³ M KCl as a function of pH.

electrodes. The zeta potential was calculated according to Smoluchowski:⁷⁷

$$\zeta = \frac{dU}{dp} \cdot \frac{\eta}{\epsilon_r \epsilon_0} \cdot \kappa \quad (6)$$

where U is the streaming potential, p is the pressure loss, ϵ_r and ϵ_0 are the dielectric constant and the vacuum permittivity, η is the viscosity, and κ the conductivity of the measuring solution.

For defined solid surfaces, electrokinetic measurements reveal the zeta potential, i.e., the electrical potential at the shear plane between the tightly adsorbed ions in the immobile part of the electrical double layer and the mobile ions in the solution. In the case of swollen polyelectrolyte brushes, the behavior is more complex. There is a significant charge near the surface of the brush and a large amount of mobile counterions inside the brush. The equilibrium between brush molecules and counterions is disturbed by the streaming solution. Therefore, no definite shear plane exists, and no zeta potential can be measured according to the definition mentioned above.⁷⁸ Electrokinetic measurements, however, yield an apparent zeta potential value which can be used at least as a relative measure of the dissociation and charging of the brushes and the sign of the charging. Figure 1 shows the apparent zeta potential of the PAA brush and the P2VP brush and the zeta potential of microsilica spheres.

AFM Force Measurements. Colloidal probes were prepared by glueing dry silica spheres (Bang Laboratories, USA, mean diameter 4.74 μ m) onto tipless silicon nitride AFM cantilevers NP-O (Veeco Instruments, Inc., USA) by a micromanipulator using a two-component epoxy resin (UHU plus endfest 300, UHU GmbH, Germany). The spring constant of each cantilever was determined before the glueing of the spheres using the thermal noise method⁷⁹ or the reference cantilever method. It was on the order of 0.5 N/m to 1.0 N/m. The results of both methods had an error of up to 20%. The effect of the glued sphere on the spring constant was within this error limit. The diameter of the spheres was determined after the measurement from scanning electron microscope images (Phenom, FEI Co., USA) with an accuracy of ± 0.05 μ m. AFM images of spheres glued to AFM cantilevers were taken by a silicon tip grating TGT 01 (MikroMasch, Estonia).⁸⁰ The image was flattened by a third-order polynomial fit to

(73) Azzam, R. M. A.; Bashara, N. M. *Ellipsometry and Polarized Light*; North Holland: Amsterdam, 1999.

(74) Ionov, L.; Zdyrko, B.; Sidorenko, A.; Minko, S.; Klep, V.; Luzinov, I.; Stamm, M. *Macromol. Rapid Commun.* **2004**, *25*, 360.

(75) Ribitsch, V.; Jorde, C.; Schurz, J.; Jacobasch, H.-J. *Prog. Colloid Polym. Sci.* **1988**, *77*, 49.

(76) Bellmann, C.; Klinger, C.; Opfermann, A.; Böhme, F.; Adler, H.-J. *Prog. Org. Coat.* **2002**, *44*, 93.

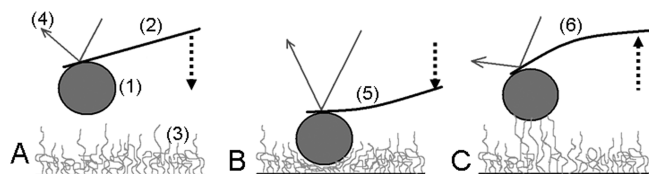
(77) Smoluchowski, M. *Handbuch der Elektrizität und des Magnetismus*; Band II; Barth-Verlag: Leipzig, 1921.

(78) Zimmermann, R.; Norde, W.; Cohen Stuart, M. A.; Werner, C. *Langmuir* **2005**, *21*, 5108.

(79) Hutter, J. L.; Bechhoefer, J. *Rev. Sci. Instrum.* **1993**, *64*, 186.

(80) Elmahdy, M. M.; Drechsler, A.; Gutsche, C.; Synytska, A.; Uhlmann, P.; Kremer, F.; Stamm, M. *Langmuir* **2009**, *25*, 12894.

Scheme 1. Principle of the AFM Colloidal Probe Measurements^a



^a A microsized sphere (1) glued to a microscopic cantilever spring (2) is approached to a brush-covered surface (3) until a maximum deflection of the cantilever is reached. Afterwards, the sphere is retracted. Repulsive and attractive forces are recorded as a function of the distance by a positive (5) or negative (6) deflection of the cantilever, which is transferred to a position-sensitive photodiode by a laser beam (4). Three possible situations are shown: A, without interaction; B, steric repulsion by the compressed brush; C, attractive interaction by adhered brush molecules during the retraction of the sphere.

determine the rms roughness of the spheres, which was ~ 2 nm over an area of $2.5 \times 2.5 \mu\text{m}^2$.

Interaction forces were measured in a MultiMode AFM with a NanoScope III Controller (Veeco Instruments, Inc., USA) equipped with a closed fluid cell at 300 ± 3 K. Before each measurement series, the silicon wafer, the colloidal probe, and the fluid cell were rinsed thoroughly with acetone, ethanol, and water and exposed to UV radiation for 20 min to remove organic contaminations. After mounting the brush sample and the colloidal probe, the cell was flushed with the electrolyte solution. 10–20 min later, when thermal equilibrium was reached, the measurement was started. The colloidal probe was approached to the brush with a speed of 300 nm/s until a certain maximum force was reached. Then, the probe was retracted with the same speed. In Scheme 1, the principle of the measurement is drawn. 256 force–distance curves were recorded in force–volume mode on a $20 \times 20 \mu\text{m}^2$ area of the surface. Care was taken to always apply the same maximum force. After each measurement, the cell was rinsed thoroughly with the next electrolyte solution and the next measurement was performed.

The measurement yields a cantilever deflection vs z position relation that gives no direct information on the distance between the colloidal probe and the surface. To obtain a force vs distance curve, the cantilever sensitivity and the distance between the probe and the surface have to be determined. In the case of hard surfaces, the measured curves show a linear slope when sphere and surface are in contact. This slope is used to determine the cantilever sensitivity and the distance and to convert the measured data into force–distance curves.⁸¹ For soft surfaces as, e.g., swollen brushes, there is no defined brush surface and no linear slope of the measured curve even if the probe and the brush are in contact. Therefore, the cantilever sensitivity was determined from force curves performed in a scratch on the brush sample or by force measurements with the same colloidal probe on a reference sample with a hard silicon oxide surface. In order to compare the curves measured with differently swollen brushes, the parameter distance was defined as the distance between the colloidal probe and the basis of the brush, i.e., surface of the silicon substrate. The distance was determined by imaging a scratch within the brush by the colloidal probe applying a definite force for each KCl solution. The height difference between the brush and the scratch yields the distance between sphere and substrate for the given solution and applied force. The force–distance curves were then shifted parallel to the distance axis until they crossed the force–distance point obtained in this way.⁵²

Usually, a majority of the curves obtained in force–volume mode coincided very well. Some of the curves showed, however, deviations due to brush defects or to interference effects of the laser beam that could not be removed by readjusting the laser. Therefore, at least 20 representative single curves were chosen for

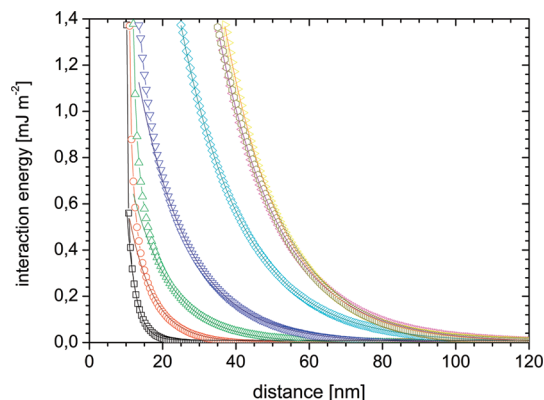


Figure 2. Interaction energy (approach curves) between a SiO_2 sphere (diameter $4.84 \pm 0.05 \mu\text{m}$) and a PAA brush in 10^{-3} M KCl. pH values (from left to right): 2.5 (black squares), 3 (red circles), 3.5 (green up triangles), 4 (blue down triangles), 5 (cyan diamonds), 6 (magenta left triangles), 7 (yellow right triangles), and 9.2 (dark yellow pentagons). The lines mark the exponential fits according to eq 5.

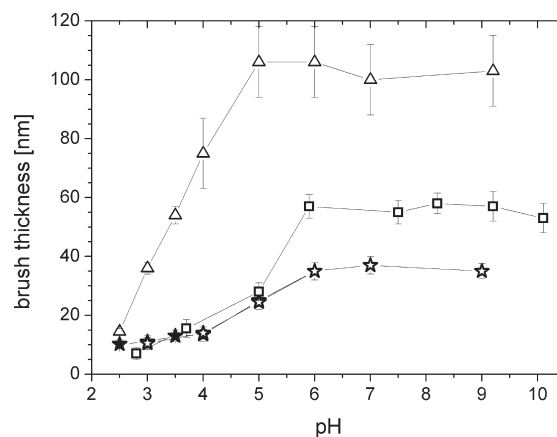


Figure 3. Thickness of PAA brushes in 10^{-3} M KCl as a function of pH determined by null-ellipsometry (squares), from AFM images (open stars, decreasing pH; full stars, increasing pH; applied force 18 ± 1 nN/ 1.1 mJ/m^2 , sphere diameter $4.84 \pm 0.05 \mu\text{m}$), and from the exponential fit to the energy–distance curves (triangles).

each concentration and averaged to reduce the influence of inhomogeneities and statistical scattering. To eliminate the influence of the sphere diameter, the force F was converted into a geometry-independent interaction energy E according to eq 3.

3. Results and Discussion

3.1. Force Measurements between SiO_2 Spheres and Poly(acrylic acid) Brushes. Influence of the pH Value. The forces between SiO_2 spheres and a PAA brush were measured in 10^{-3} M KCl solutions. The pH value was stepwise decreased from pH = 9.2 to pH = 2.5. To ensure the reversibility of the process, the pH was increased afterward to pH = 7. In Figure 2, the interaction energy calculated according to eq 3 is shown for decreasing pH values. There is no significant difference between the curves measured with decreasing pH and those with increasing pH. Due to the uncertainty of the determination of the spring constant (up to 20%), only results obtained with the same colloidal probe are compared. Other measurements confirm these results, however, with a systematic error.

The position of the curves relative to the distance axis was determined by measuring the thickness of the brush from the

(81) Senden, T. J. *Curr. Opin. Colloid Interface Sci.* **2001**, *6*, 95.

Table 1. Decay Length t_1 and Thickness L of PAA Brushes Obtained from the Exponential Fit of the Interaction Energies in Figure 2 (in 10^{-3} M KCl solution) and the Debye Length κ^{-1} Calculated for the Given Total Ion Concentration (KCl + HCl/KOH)

pH	t_1 [nm]	κ^{-1} [nm]	L [nm]
2.5	2.3 ± 0.2	4.71	14.5 ± 1
3	5.8 ± 0.4	6.80	36 ± 2
3.5	8.6 ± 0.5	8.38	54 ± 3
4	12 ± 1	9.17	75 ± 6
5	17 ± 1	9.57	106 ± 6
6	17 ± 1	9.61	106 ± 6
7	16 ± 1	9.61	100 ± 6

AFM image of a scratch made with a given applied force as described in the Experimental section. Figure 3 shows the brush thickness obtained in this way in comparison to the brush thickness measured by null ellipsometry. Both methods yield an increase of the brush thickness with growing pH value, which is typical for annealed polyacid brushes.⁴² For the swollen brushes, the AFM measurement yields lower thickness values than null ellipsometry, since the brush is compressed by the applied force.

The interaction energy E between the PAA brush and the silica sphere (Figure 2) shows for all pH values a clearly repulsive behavior. The range and strength of the repulsion increase with increasing pH value. This reflects qualitatively the swelling of the brush. For $\text{pH} \geq 6$, the pH has no influence on the interaction; the energy–distance curves are identical within the limits of experimental error.

The curves were modeled by an exponentially decaying function according to eq 5. The fits are shown as solid lines in Figure 2. The exponential decay length t_1 is a measure of the range of the interaction energy. In the case of a pure electrostatic interaction, it equals the Debye length, which can be calculated directly from the salt concentration and the valence of the ions in the solution.⁸² For apparently uncharged brushes, the brush thickness can be estimated from the decay length according to eq 5. In Table 1, the decay length t_1 , the calculated Debye length for the given total (KCl + HCl/KOH) ion concentration, and the brush thickness L obtained from the energy–distance curves in Figure 2 are listed. At pH values $2.5 \leq \text{pH} \leq 3.5$, the decay length t_1 is approximately on the order of the Debye length. In this pH range, the brush is undissociated and collapsed; the interaction is mainly electrostatic. Increase of the pH value causes a dissociation and swelling of the brush. The decay length grows up to 17 nm for the completely dissociated and swollen brush at $\text{pH} \geq 6$. Here, it is significantly higher than the Debye length; the repulsive force may not be interpreted as a pure electrostatic interaction but as a steric interaction of the swollen brush.

The brush thickness L calculated from t_1 according to eq 5 yields, however, values that are significantly larger than the thickness determined by ellipsometry (cf. Figure 3). This may be for the following reasons: (1) The interaction is neither a pure steric repulsion by the brush molecules nor a pure electrostatic repulsion, but a combination of both. Both contributions cannot be separated by simple arithmetic models, since each molecule chain of the brush interacts via both mechanisms with the microsized sphere. (2) The brush may not have a defined surface as assumed in the ellipsometry model but may consist of a dense layer from which single molecules extend into the solution as suggested by Block and Helm.^{56,57} Ellipsometry measurements may detect only the dense region with a refractive index different

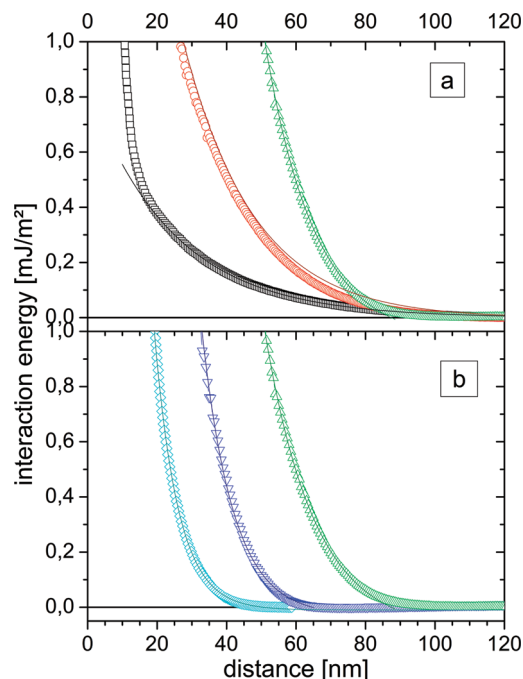


Figure 4. Interaction energy (approach curves) between a SiO_2 sphere (diameter $4.81 \pm 0.05 \mu\text{m}$) and a PAA brush at pH 6.8. (a) in osmotic brush regime, KCl concentrations (from left to right): 10^{-4} M (black squares), 10^{-3} M (red circles), 10^{-2} M (green up triangles). (b) in salted brush regime, KCl concentrations (from left to right) 1 M (cyan diamonds), 0.1 M (blue down triangles), 10^{-2} M (green triangles). The lines mark the exponential fits according to eq 5.

from that of the solution, but not single molecules. Therefore, single stretched chains may interact sterically beyond the brush thickness measured by ellipsometry. This effect seems to be especially pronounced in the pH range between 3 and 5 where the brush is only partly dissociated. Due to the lower counterion density in the surrounding solution, these stretched molecules might be more dissociated than the molecules in the bulk. This is, however, only a vague assumption that has to be tested by complementary methods as, e.g., neutron scattering^{83,84} or by analytical models, e.g., those used for the modeling of the interaction between proteins and polyelectrolyte brushes.^{15,16,40}

No attractive forces have been observed at any pH. The reason for this is that PAA brushes and SiO_2 have a comparable pH dependence of the surface potential (cf. Figure 1). Obviously, patches of different charge as known for proteins^{15,16,40} do not exist on the brush or silica surface. Therefore, no electrostatic attraction occurs. Other attractive forces as van der Waals or dipole forces are suppressed by the steric and electrostatic repulsion of the brush that avoids a close contact of the surfaces.

The interaction between two microsized silica spheres covered with PAA brushes similar to those used in this study has been measured by Dominguez et al. using optical tweezers.⁵⁸ They also observed purely repulsive forces that reflect the swelling of the brush with increasing pH.

Influence of the Salt Concentration. Figure 4 shows the interaction energy between the PAA brush and a SiO_2 sphere in KCl solutions of varying concentration at pH 6.8. At all concentrations, a repulsive behavior is observed. Table 2 summarizes the decay length of this repulsion, the Debye length for the given

(82) Israelachvili, J. N. *Intermolecular and Surface Forces*, 2nd ed.; Academic Press: San Diego, 1991.

(83) Mir, Y.; Auroy, P.; Auvray, L. *Phys. Rev. Lett.* **1995**, 65, 2863.

(84) Tran, Y.; Auroy, P.; Lee, L.-T.; Stamm, M. *Phys. Rev. E* **1999**, 60, 6984.

Table 2. Decay Length t_1 and Thickness L of PAA Brushes Obtained from the Exponential Fit of the Interaction Energies in Figure 4 (at pH = 6.8) and the Theoretical Debye Length κ^{-1} for the Given Total Ion Concentration (KCl + KOH)

KCl conc. [mol/L]	t_1 [nm]	κ^{-1} [nm]	L [nm]
1×10^{-4}	24.2 ± 1	30.4	152 ± 6
1×10^{-3}	20 ± 1	9.61	125 ± 6
0.01	9.7 ± 0.3	3.04	61 ± 2
0.1	7.7 ± 0.2	1.03	48 ± 1
1	6.8 ± 0.2	0.30	43 ± 1

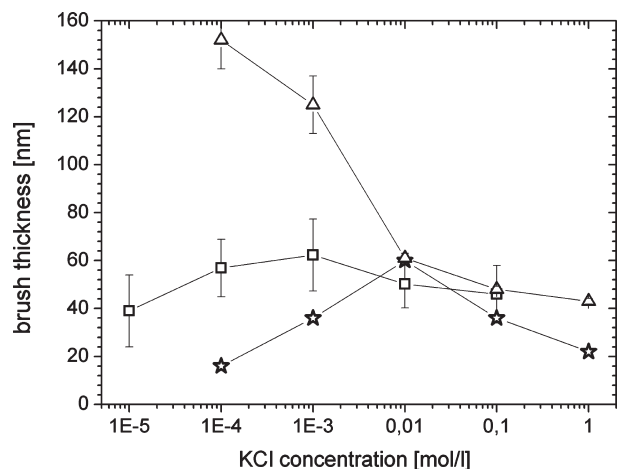


Figure 5. Thickness of PAA brushes as a function of the KCl concentration determined by null ellipsometry (squares, pH 5.9), from AFM images (stars, applied force 10 ± 1 nN/ 0.66 mJ/m², sphere diameter 4.81 ± 0.05 μ m; pH 6.8) and from the exponential fit to the energy–distance curves (triangles, pH 6.8).

concentrations, and the brush thickness obtained from the decay length. The Debye lengths are slightly lower than the theoretical values for the given concentrations due to the addition of KOH to adjust the pH value. In Figure 5, the values of the brush thickness obtained from the image of a scratch and from the exponential fit of the curves are compared to the thickness measured by ellipsometry.

Figure 4a shows the energy–distance curves in the concentration range between 10^{-4} M and 10^{-2} M KCl. Here, the brush is in the osmotic regime. Increasing the ionic strength leads to an increasing osmotic pressure within the brush. This is reflected in Figure 4a by an increasing range and strength of the repulsive interaction. In the 10^{-4} M solution, the interaction energy is rather weak but decays slowly with a decay length t_1 of about 24 nm. This value is near the theoretical Debye length of 30.4 nm. Thus, the interaction may be considered a mostly electrostatic interaction of an only slightly swollen brush. If the KCl concentration is increased up to 10^{-3} M and 10^{-2} M, the repulsion becomes stronger. Its decay length decreases to about 10 nm, which is significantly higher than the Debye length (cf. Table 2); the interaction must be considered as a combined electrostatic and steric repulsion. Interestingly, in all concentrations within the osmotic brush regime, the repulsion extends up to a distance of about 100 nm, which refers approximately to the contour length of the PAA molecules. The brush thickness calculated from the decay length has no relation at all to the thickness obtained by other methods (cf. Figure 5). Obviously the Alexander de Gennes model cannot be applied in the osmotic brush regime. More specific calculations, e.g., by self-consistent field analysis⁴⁰ are needed to model this behavior.

If the KCl concentration is increased further, the brush enters the salted regime (cf. Figure 4b). Here, the charge of the

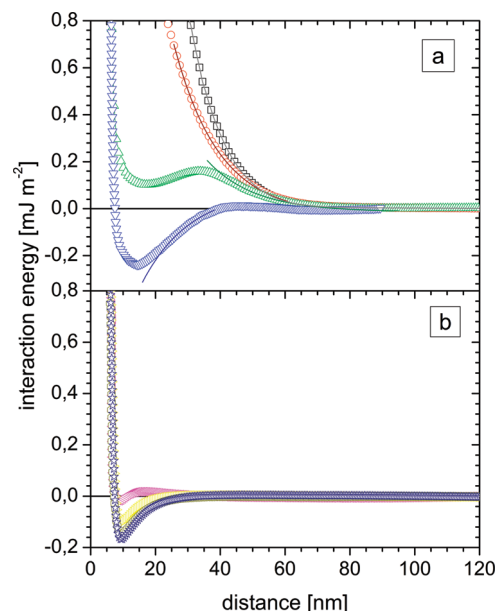


Figure 6. Interaction energy (approach curves) between a SiO₂ sphere (diameter 4.77 ± 0.05 μ m) and a P2VP brush in 10^{-3} M KCl. (a) pH values (from top to bottom): 2.5 (black squares), 3 (red circles), 3.5 (green up triangles), and 4 (blue down triangles). (b) pH values: 5 (magenta left triangles), 6 (yellow right triangles), 7 (dark yellow pentagons), and 8 (dark blue stars). The lines mark the exponential fits according to eq 5.

polyelectrolyte molecules is screened by the ions of the solution. The brush shrinks with growing concentration. This can be seen in Figure 4b by the decreasing range of the interaction energy. The decay length decreases only slightly with increasing concentration. It is much higher than the Debye length. The brush thickness obtained from the exponential fit of the energy–distance curves is close to the values obtained by ellipsometry. It can be concluded that the interaction in the salted brush regime can be described appropriately by the Alexander de Gennes model.

Both ellipsometry and AFM investigations give a maximum of the brush thickness that is typical for annealed brushes.^{2,42} The position of the maximum differs slightly due to the different pH values used in ellipsometry and AFM measurements.

In the force measurements between two microsized spheres with grafted PAA brushes, Dominguez et al.⁵⁸ observed a different behavior. The range and strength of the repulsive interaction decreased monotonically with increasing salt concentration. Separation of electrostatic and steric forces and modeling according to Jusufi⁸⁵ yielded, however, a maximum of the steric interactions in 10^{-4} M KCl solutions. In addition, for various salt concentrations, no attractive forces have been observed due to the similar charging of the PAA brush and SiO₂ as discussed above.

3.2. Force Measurements between SiO₂ Spheres and Poly(2-vinyl pyridine) Brushes. Influence of the pH Value.

The interaction between a P2VP brush and a SiO₂ sphere in 10^{-3} M KCl solution during the approach of the sphere is shown in Figure 6. During this measurement, the pH value was increased stepwise from pH = 2.5 to pH = 8. In contrast to the PAA brush, the P2VP brush acts purely repulsively only at pH = 2.5. At this pH, the brush is completely protonated and swollen, while the silica sphere is nearly uncharged. The repulsive force may thus be interpreted as a purely steric repulsion caused by the osmotic pressure of the swollen brush. A similar but weaker repulsion is

(85) Jusufi, A.; Likos, C. N. *J. Chem. Phys.* **2006**, *124*, 214904.

Table 3. Decay Length ℓ_1 and Thickness L of P2 VP Brushes Obtained from the Exponential Fit of the Interaction Energies in Figure 6 (in 10^{-3} M KCl solution) and the Debye Length κ^{-1} Calculated for the Given Total Ion Concentration (KCl + HCl/KOH)

pH	ℓ_1 [nm]	κ^{-1} [nm]	L [nm]
2.5	9 ± 0.8	4.71	56 ± 5
3	12 ± 1	6.80	75 ± 6
3.5	13 ± 1	8.38	81 ± 6
4	15 ± 1	9.17	93 ± 6
5	-;	9.57	-;
6	5.2 ± 0.3	9.61	
7	5.9 ± 0.4	9.61	
8	6.3 ± 0.4	9.61	

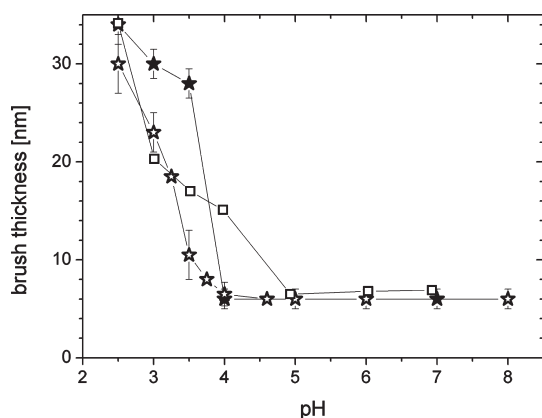


Figure 7. Thickness of P2 VP brushes in 10^{-3} M KCl as a function of pH determined by null ellipsometry (open squares) and by AFM force measurements (open stars, increasing pH; full stars, decreasing pH; applied force 11 ± 1 nN/ 0.73 mJ/m², sphere diameter 4.77 ± 0.05 μ m).

observed at pH = 3. If the pH value is increased up to pH = 3.5, the repulsive force is overlapped by an increasing attractive force. At pH = 4, the attractive force dominates the interaction. Since the zeta potential of the P2 VP brush and SiO₂ have different signs between pH = 2.8 and pH = 6.7, this force is assumed to be based on electrostatic effects. From the exponential fit of the outer parts of the curves (solid lines in Figure 6), the decay length and the thickness of the brushes was calculated (Table 3). The decay length is always higher than the theoretical Debye length. The brush thickness calculated from the exponential fit (Table 3) is much higher than that obtained by ellipsometry and AFM imaging (shown in Figure 7) and seems to increase with increasing pH value. Obviously, the brush does not behave like a swollen, uncharged brush and thus cannot be modeled by the Alexander de Gennes model. In contrast, the interaction is a very complex interplay of electrostatic and steric contributions of a brush layer with an inhomogeneous dissociation and swelling of the brush molecules as has been discussed above for PAA brushes. It would be very interesting to model these interactions, e.g., by self-consistent field analysis.

It must be noted that the transition from repulsive to attractive behavior has been observed only when the pH value was increased during the experiment. In force measurements performed with decreasing pH value, no attractive force was observed during the approach of the sphere. We attribute this to contaminations of the sphere or the brush due to attractive forces at higher pH values. In AFM images made at high pH values, often artifacts caused by contaminations have been observed. Furthermore, a stronger swelling of the brush was found if the pH value was decreased (Figure 7, full stars) than in experiments starting

with pH = 2.5 with increasing pH (open stars). This may be evidence for a contamination of the sphere. A similar effect was observed, however, by other researchers.⁷¹ It will be subject to further investigations.

If the pH is increased to pH > 4 (Figure 6b), only a weak attractive force becomes visible. At first glance, this seems to be an electrostatic attraction between the positively charged P2VP brush and the negatively charged silica sphere. Surprisingly, the attraction becomes stronger for pH = 7 and pH = 8 when both surfaces are negatively charged. Adhesion measurements between silica particles and P2VP brushes²⁴ confirm this attraction. The decay length of the attractive force is about 5 to 6 nm (cf. Table 1) and thus lower than the Debye length (9.6 nm).⁸² Therefore, we assume that it is rather due to specific interactions between the pyridyl groups and the silica as hydrogen bonding and van der Waals forces. It must be noted that the negative charge of the surfaces at high pH values is caused by adsorption of ions from the surrounding solution. During the approach of the sphere, the ion adsorption layer may reorganize. Thus, also entropic effects may be responsible for the attractive force. At distances ≤ 8 nm, which correspond to the dry thickness of the brush, a steep steric repulsion by the compressed brush is observed.

The attractive forces between P2VP and silica are more obvious if the sphere is retracted from the brush. For all pH values except pH = 2.5, an adhesion force was observed after the sphere and the brush had been in contact, even if there is no attractive force visible on approach. The absolute value of this adhesion force varied between the different measurement series. Nevertheless, in all measurements a maximum adhesion was observed between pH = 3.5 and pH = 4. At pH ≥ 5 , the adhesion remained constant at about 70% of the maximum value. A detailed discussion of the adhesion of silica particles on P2VP brushes is given in a separate paper.

Figure 7 compares the thickness of the brush as determined by null ellipsometry and from the AFM image of a scratch with an applied force of 11 nN (0.7 mJ m⁻²). Both curves point out the swelling of the P2VP brush at pH = 2.5 and the deswelling if the pH value is increased. The thickness obtained from the AFM images for pH = 2.5 and pH ≥ 5 corresponds well with the values measured by null ellipsometry. At these pH values, the brush shows a steeply decaying repulsive force and is only slightly compressed by the colloidal probe. In the range between pH = 3 and pH = 5, the repulsive force is weaker; the brush is compressed significantly by the probe leading to a difference of the thickness obtained by both methods. As discussed above, a stronger swelling is observed when the pH value is decreased.

Similar force-distance measurements have been performed between two micro-sized spheres covered with a comparable P2 VP brush using optical tweezers.⁵⁹ Between two like brush-covered spheres, only repulsive forces act. They reflect a full swelling of the brush at pH < 4 and a transition to lower brush heights at increasing pH. This shows that the geometry of the brush has a significant influence on the pH dependence of the swelling.

Influence of the Salt Concentration. The influence of the salt concentration on the interaction between a P2VP brush and a SiO₂ sphere was determined at various pH values. At pH = 7, when the brush is collapsed, the salt concentration does not affect the interaction forces. At all salt concentrations, curves similar to that shown in Figure 6 for pH 7 and 8 were measured.

At pH = 2.5 when the brush is completely protonated, the salt concentration affects the interaction forces as can be seen in Figure 8. It must be noted that, due to the adjustment of the pH by HCl, the counterion (Cl⁻) concentration is already 3.16×10^{-3} M without addition of KCl. Thus, the brush is already in the salted

brush regime at the lowest KCl concentration. Increasing the added amount of KCl makes the brush shrink. The decay length decreases but is always significantly higher than the Debye length predicted for the solutions (cf. Table 4). It is thus postulated that the forces represent a steric interaction of the swollen brush. Since the SiO₂ sphere is nearly uncharged at pH = 2.5 (cf. Figure 1), no electrostatic interactions are expected.

If the KCl concentration is increased to 1 M, the brush is not only compressed, but there is additionally a significant attractive force at distances between 35 and 55 nm. This force was reproduced in several experiments. It must be of the same origin as the attractive force at pH \geq 5, i.e., due to specific interactions between the pyridyl groups of the P2VP brush and the polar silica surface. While retracting the brush, already at a salt concentration of 0.1 M a weak adhesion was observed. In 1 M solutions, the adhesion force was on the order of 20 nN in the measurements shown in Figure 8. It must be noted, however, that the absolute value of the adhesion force depends strongly on the maximum applied force but is affected also by the history of the brush, the size of the silica particle, and other factors.

Figure 9 compares the brush thickness calculated according to eq 5 with the data obtained by ellipsometry and from an AFM image of a scratch in the brush. All three methods show the typical shrinking of a polyelectrolyte brush with increasing salt concentration in the salted regime. At Cl[−] concentrations of <0.01 M, the modeling according to eq 5 yields higher values of the brush thickness than the AFM image of a scratch. That reflects the compression of the brush during the AFM image. At higher

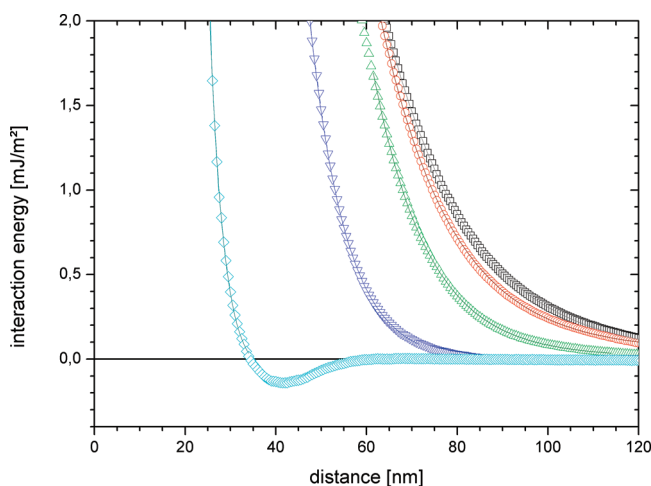


Figure 8. Interaction energy (approach curves) between a SiO₂ sphere (diameter $4.27 \pm 0.05 \mu\text{m}$) and a P2VP brush in at pH 2.5. Cl[−] (KCl+HCl) concentrations (from right to left): 3.26×10^{-3} M (black squares), 5.16×10^{-3} M (red circles), 1.32×10^{-2} M (green up triangles), 0.103 M (blue down triangles), 1 M (cyan diamonds). The lines mark the exponential fits according to eq 5.

concentrations, the repulsive force becomes stronger. Thus, the brush is less compressed by the sphere. Interestingly, ellipsometry gives lower brush thicknesses for the swollen brush than AFM measurements. This might be a consequence of different measurement conditions. In various experiments, it has been found that P2VP brushes are very sensitive to small differences in the preparation and storing of the brush as well as of the experimental setup.

Interestingly, optical tweezers force measurements between two silica spheres carrying P2VP brushes show no influence of the salt concentration on the interaction forces at pH = 2⁵⁹—additional evidence that the geometry of the brush influences its behavior.

At pH = 4, increasing the salt concentration changes the interaction dramatically (Figure 10). Figure 10a shows the force–distance curves measured in the osmotic brush regime. In 10^{-4} M solutions, a weak repulsion acts between the brush and the SiO₂ sphere followed by a slight jump-in near the brush surface. In 10^{-3} M solutions, the interaction has changed completely. Now, a long-range attractive force governs the interaction. In 2×10^{-3} M KCl, the curve may be interpreted as a combination of a repulsive interaction with a range up to 80 nm and a strong attractive interaction at distances up to 50 nm. It is an interesting fact that, despite the different surface charge of the sphere and the brush in this pH region, a non-negligible repulsive force has to be overcome before the sphere is attracted electrostatically by the brush molecules. The shape of the interaction energy curve

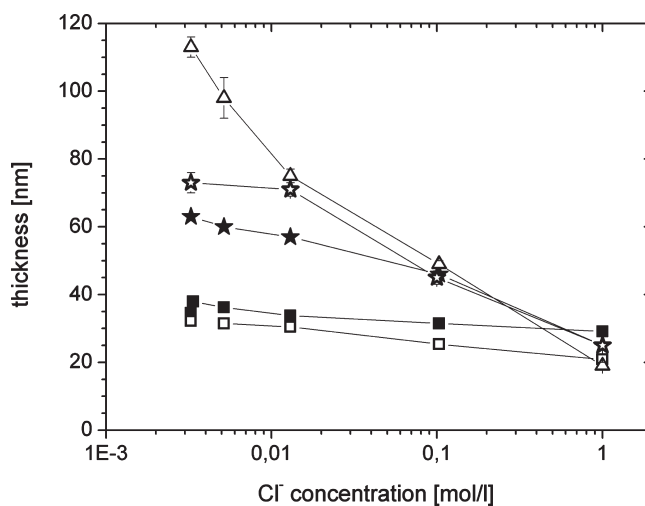


Figure 9. Thickness of P2VP brushes at pH = 2.5 as a function of Cl[−] (KCl + HCl) concentration determined by null ellipsometry (open and full squares, two measurement series), by AFM force measurements (full stars, increasing Cl[−] concentration; open stars, decreasing Cl[−] concentration; applied force 30 ± 1 nN; sphere diameter $4.90 \pm 0.05 \mu\text{m}$) and from the exponential fit to the energy–distance curves (triangles).

Table 4. Decay Length τ_1 and Thickness L of P2VP Brushes Obtained from the Exponential Fit of the Interaction Energies in Figures 8 and 10 and Theoretical Debye Length κ^{-1} for the Given KCl Concentrations

KCl conc. [mol/L]	pH 2.5 τ_1 [nm]	κ^{-1} [nm]	L [nm]	pH 4 τ_1 [nm]	κ^{-1} [nm]	L [nm]
1×10^{-4}	18.5 ± 0.5	5.32	113 ± 3	15.8 ± 0.8	21.5	99 ± 5
1×10^{-3}	–	–	–	10.7 ± 1	9.17	67 ± 6
2×10^{-3}	15.8 ± 0.5	4.23	98 ± 6	9.7 ± 0.2	6.63	61 ± 1
4×10^{-3}	–	–	–	11.1 ± 0.7	4.75	70 ± 5
1×10^{-2}	11.9 ± 0.3	2.65	75 ± 2	16.5 ± 0.5	3.02	104 ± 3
0.1	8.0 ± 0.2	0.95	49 ± 1	10.0 ± 0.3	0.96	62 ± 2
1	3.1 ± 0.2	0.30	19 ± 1	4.0 ± 0.2	0.30	25 ± 1

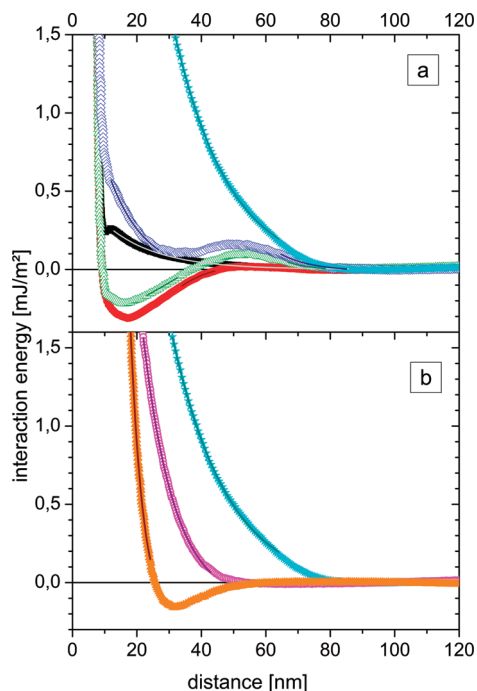


Figure 10. Interaction energy (approach curves) between a SiO₂ sphere (diameter $4.94 \pm 0.05 \mu\text{m}$) and a P2VP brush at pH 4. (a) KCl concentrations: 10^{-4} M (black squares), 10^{-3} M (red circles), 2×10^{-3} M (green up triangles), 4×10^{-3} M (blue diamonds), and 10^{-2} M (cyan stars). (b) KCl concentrations (from right to left): 10^{-2} M (cyan stars), 0.1 M (magenta circles), and 1 M (orange triangles).

measured in 4×10^{-3} M KCl solution is caused by the same contributions, but now the repulsive and the attractive force are nearly equivalent. In 10^{-2} M KCl solution, the P2VP brush shows the same purely repulsive behavior of a completely swollen brush as at pH = 2.5. The change of the curves represents the transition of the brush from the osmotic brush regime at low salt concentrations to the salted brush regime in 10^{-2} M solutions.

If more salt is added, the brush enters the salted regime (Figure 10b). Now, an increase of the salt concentration leads similar to pH 2.5 to a shrinking of the brush. In 1 M KCl solutions, again an attractive force with a maximum at distances around 30 nm is observed.

During the retraction of the probe, in all solutions at pH = 4 an adhesion force was observed. In the experiment shown in Figure 10, it increased from 12 ± 4 nN in 10^{-4} M KCl to nearly 100 nN in the 4×10^{-3} M KCl solution. Further increase of the KCl concentration diminished the adhesion to 16 ± 2 nN in 0.1 M KCl. In 1 M KCl, again a stronger adhesion of 35 ± 4 nN was observed. These values show that the adhesion force between silica particles and P2VP brushes can be varied significantly by changing the salt content of the surrounding solution.

The energy–distance curves shown in Figure 10 were modeled, too, by an exponential decay function according to eq 5 (solid lines in Figure 10). The decay length, the theoretical Debye length, and the brush thickness obtained from the fit are shown in Table 4. A coarse agreement between the decay length and the Debye length is obtained for the repulsive force in 10^{-4} M KCl and for the attractive force in 10^{-3} M KCl. This may be evidence that these forces are mainly electrostatic interactions between a mostly collapsed brush and the silica particle. For all other KCl concentrations, the interaction is a complex interplay of different contributions that cannot be described by simple electrostatic and steric models. Figure 11 compares the thickness values obtained

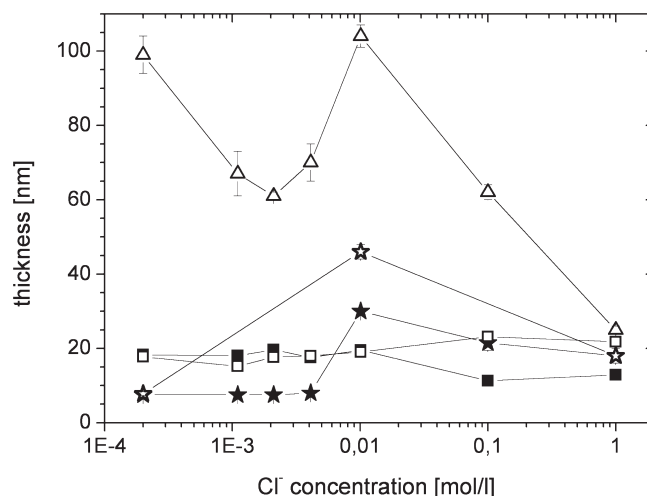


Figure 11. Thickness of P2VP brushes at pH = 4 as a function of the Cl[−] (KCl + HCl) concentration determined by null ellipsometry (squares, two measurement series), by AFM force measurements (full stars, increasing Cl[−] concentration; open stars, decreasing decreasing Cl[−] concentration; applied force 30 ± 1 nN; sphere diameter $4.33 \pm 0.05 \mu\text{m}$) and from the exponential fit to the energy–distance curves (triangles).

by the modeling, the AFM image of a scratch, and ellipsometry. The brush thickness obtained from the fits shows only in the salted brush regime the same tendency as the other methods but is always higher than the values obtained by ellipsometry and from the AFM images of a scratch in the brush except for the highest salt concentration. In the osmotic brush regime, rather unrealistic values are computed. Due to the very complex interactions, the Alexander de Gennes model is not suitable to model these force–distance curves.

Optical tweezers force measurements between two P2VP covered silica spheres at pH = 4⁵⁹ revealed a quite different behavior. Due to the same surface charge of the two spheres, no attractive forces occur. Only a compression of the brushes is observed when the KCl concentration exceeds 10^{-3} M.

4. Conclusions

The interaction forces between micro-sized SiO₂ spheres and annealed polyelectrolyte brushes made of the weak polyacid poly(acrylic acid) (PAA) or the weak polybase poly(2-vinyl pyridine) (P2VP) have been measured using the AFM colloidal probe technique in situ in KCl solutions of varying pH and ionic strength. It has been shown that AFM force measurements are a suitable method to elucidate the swelling of the brushes and the variation of the interaction forces in various aqueous environments with high accuracy.

If the brushes are swollen and in the salted brush regime (for PAA at basic pH and at high salt concentrations, for P2VP at low pH and high salt concentrations), they exhibit a strong steric repulsion that acts up to distances comparable with the contour length of the brush molecules. This repulsion can be described approximately using the Alexander de Gennes model for uncharged brushes.

In the osmotic brush regime (i.e., when the brush is at least partly swollen but the salt concentration is low), the behavior is more complicated. In the case of PAA brushes, the repulsion becomes weaker but acts at about the same distance as in the salted regime. With P2VP, an additional strong attractive force comes into play due to the different charges of the brush and the micro-sized sphere. This behavior is assumed to be a complex

interplay of steric and electrostatic forces between the micro-sized sphere and differently stretched polyelectrolyte molecules. A theoretical description is difficult and will be the subject of further work.

In the pH range where the brush is collapsed ($\text{pH} = 2.5$ for PAA, $\text{pH} > 5$ for P2VP), a strong steric repulsion is observed for distances that are lower than or equal to the dry thickness of the brush. At larger distances, a weak repulsion is detected between PAA and the SiO_2 sphere, which have nearly the same surface charge. Between the P2VP brush and the SiO_2 sphere, an attractive force acts, even in the pH range where both surfaces are negatively charged. A comparable attractive force between P2VP brushes and silica spheres was observed in 1 M KCl solutions, but at somewhat larger distances.

Between the PAA brush and the SiO_2 sphere, no attractive forces have been found at any pH or salt concentration. In contrast, P2VP brushes exert a strong adhesive force on the SiO_2 sphere except in solutions with $\text{pH} = 2.5$ and KCl concentrations of < 0.1 M. A maximum adhesion has been found in solutions with pH values between $\text{pH} = 3.5$ and $\text{pH} = 4$ and KCl concentrations between

10^{-3} M and 10^{-2} M, i.e., when the brush is in the osmotic brush regime and partly swollen. However, if the brushes are collapsed at high pH values and salt concentrations, adhesion forces have been observed between them and the SiO_2 particles.

Comparison with force measurements between two silica spheres covered with grafted PAA or P2VP brushes showed that the geometry of the interacting surfaces has a significant influence on the pH-dependent swelling and interaction of the brushes.

Acknowledgment. Financial support for this work provided by the Deutsche Forschungsgemeinschaft DFG (Projects STA 324/33-1, KR 1138/20-1 and SY 125/1-1) is gratefully acknowledged. The Authors would also like to thank T. Riske, D. Nitsche, and C. Hase for the preparation of the brushes, C. Hase for ellipsometric measurements and A. Caspari for the zeta potential measurements.

Supporting Information Available: Additional information as described in the text. This material is available free of charge via the Internet at <http://pubs.acs.org>.